

Risk-averse decision strategies for influence diagrams using rooted junction trees

Olli Herrala^a, Topias Terho^a, Fabricio Oliveira^{a,*}

^aDepartment of Mathematics and Systems Analysis, Aalto University, School of Science, FI-00076 Aalto, Finland

Abstract

This paper presents how a mixed-integer programming (MIP) formulation for influence diagrams, based on a gradual rooted junction tree representation of the diagram, can be generalized to incorporate risk considerations such as conditional value-at-risk and chance constraints. We present two algorithms on how targeted modifications can be made to the underlying influence diagram or to the gradual rooted junction tree representation to enable our reformulations. We present computational results comparing our reformulation with another MIP formulation for influence diagrams.

Keywords: influence diagram, mixed-integer programming, risk-aversion

1. Introduction

An influence diagram (ID) [11] is an intuitive structural representation of a decision problem with uncertainties and interdependencies between random events, decisions and consequences. Traditional solution methods for influence diagrams [24] often require strong assumptions such as the no-forgetting assumption. Lauritzen and Nilsson [16] present the notion of a limited memory influence diagram (LIMID) that, albeit more general in terms of representation capabilities, does not satisfy the no-forgetting assumption and, therefore, is not amenable to these traditional methods.

The algorithms presented in the literature for solving decision problems represented as IDs are mostly suited only to problems where an expected utility function is maximized and risk is not explicitly constrained. Thus, often risk considerations are encoded in the utility function itself, by making it concave using, e.g., utility extraction techniques [4, 8, 19].

Very often, utility functions represent monetary values, such as costs or revenues. In that case, maximizing expected utility assumes that the decision-maker has a risk-neutral stance. However, decision-makers may still have different risk tolerance profiles, which must be represented in the decision process.

There are numerous ways to incorporate risk aversion into decision models without requiring utility extraction techniques. A typical method is to minimize a risk measure instead of expected utility [18]. A commonly used measure is the *conditional Value-at-Risk* (CVaR), which measures the expected loss value in the α -tail, α being a confidence level parameter [21]. Another typical way of incorporating risk aversion is to use constraints such as those related to chance events or budget violations [2]. Both mentioned methods have been used widely in various applications (See, e.g., [6, 13, 26]). Directly optimizing a risk measure within an influence diagram is challenging as,

unlike expected utility, it prevents the use of methods that construct the optimal strategy by computing locally optimal strategies at individual decision nodes.

Recently, two different mixed-integer programming (MIP) reformulations for influence diagrams have emerged, likely stemming from the considerable computational improvements in MIP solution methods. The reformulation considered in this paper is originally presented by Parmentier et al. [20], where the authors first show how to convert a LIMID representing an expected utility maximization problem into a gradual rooted junction tree. This junction tree consists of clusters of nodes from the LIMID and is reformulated as a MIP problem using marginal probability distributions of nodes within each cluster. However, Parmentier et al. [20] only consider expected utility maximization and do not show how risk can be accounted for in their formulation.

In contrast, Salo et al. [22] present decision programming, which reformulates a LIMID as a mixed-integer linear programming (MILP) formulation without the intermediate clustering step of forming a junction tree. The decision programming formulation used in this paper is the one presented in [10], which improves that originally proposed in [22] by means of valid inequalities and reformulations.

The main advantage of decision programming is that its formulation can be adapted to minimize (conditional) value-at-risk, and its path-based MILP formulation makes considering different constraints straightforward, as discussed by Hankimaa et al. [10]. However, flexibility comes at a cost of computational efficiency compared to the rooted junction tree models in [20], which is demonstrated in our computational experiments.

Against this backdrop, this paper presents how the risk measures and constraints in [22] can be incorporated into the rooted junction tree model, which significantly reduces computational time compared to solving risk-averse decision strategies with decision programming. To enable our main contribution, the rooted junction tree from which the MIP is generated needs to have a specific structure. We present how rooted junction trees

*Corresponding author: fabricio.oliveira@aalto.fi

can be modified to achieve said structure. We also show that this can be achieved indirectly by modifying the underlying influence diagram, which we see as more convenient from a user’s standpoint.

In Section 2, we present background on (limited memory) influence diagrams and the MIP reformulations of such diagrams. Section 3 continues with extending the rooted junction tree-based reformulation to consider different risk measures and constraints and Section 4 presents computational results. Finally, Section 5 concludes the paper with ideas on future research directions and the potential of reformulating influence diagrams as MIP problems.

2. Background

2.1. Pig farm problem

The pig farm problem is an example of a partially observable Markov decision process (POMDP) and is used throughout this paper as the running example to illustrate the proposed developments. Cohen and Parmentier [3] further discuss the modelling of POMDPs using the methodology from Parmentier et al. [20], but we keep our focus on the more general formulations presented in the latter.

In the pig farm problem [16], a farmer is raising pigs for a period of four months after which the pigs will be sold. During the breeding period, a pig may develop a disease, which negatively affects the retail price of the pig at the time they are sold. In the original formulation, a healthy pig commands a price of 1000 DKK and an ill pig commands a price of 300 DKK. During the first three months, a veterinarian visits the farm and tests the pigs for the disease. The specificity (or true negative rate) of the test is 80%, whereas the sensitivity (true positive rate) is 90%. Based on the test results, the farmer may decide to inject a medicine, which costs 100 DKK. The medicine cures an ill pig with a probability of 0.5, whereas an ill pig that is not treated is spontaneously cured with a probability of 0.1. If the medicine is given to a healthy pig, the probability of developing the disease in the subsequent month is 0.1, whereas the probability without the injection is 0.2. In the first month, a pig has the disease with a probability of 0.1.

2.2. Influence Diagrams

An influence diagram is a directed acyclic graph $G = (N, A)$, where N is the set of nodes and A is the set of arcs. Let $N = N^C \cup N^D \cup N^V$ be the set of chance nodes N^C , value nodes N^V and decision nodes N^D in the influence diagram. Let $I(j), j \in N$, denote the information set (or parents) of j , i.e., nodes from which there is an arc to j . It is typical to assume that value nodes are not parents of other nodes. Influence diagrams can intuitively represent complex decision problems with multiple periods, each containing multiple (possibly interdependent) decisions and chance nodes. For a selection of examples, see [10, 16, 20].

Each node $j \in N$ has a discrete and finite state space S_j representing possible outcomes $s_j \in S_j$. Typically, state spaces can

have any discrete number of alternatives, as evidenced in the examples in [10, 11, 20]. For a subset of nodes $C \subseteq N$, the state space and the realized outcome are defined as $S_C := \times_{c \in C} S_c$ and $s_C = (s_c)_{c \in C}$, respectively. The outcome (i.e., state) s_j of a stochastic node $j \in N^C \cup N^V$ is a random variable with a probability distribution $\mathbb{P}(s_j | s_{I(j)})$, which corresponds to the probability of node j being in state s_j given that the parents $I(j)$ are in state $s_{I(j)}$. We denote $\mathbb{P}_G(s_j | s_{I(j)})$ when we want to emphasize that the probability distribution is associated with diagram G . The outcome of a decision node $d \in N^D$ is determined by a *decision strategy* $\delta(s_d | s_{I(d)}) : S_{I(d)} \times S_d \rightarrow \{0, 1\}$, where $\delta(s_d | s_{I(d)}) = 1$ means that state s_d is selected if nodes $I(d)$ are in states $s_{I(d)}$. A *feasible decision strategy* is such that for each $s_{I(d)} \in S_{I(d)}$, exactly one element $s_d \in S_d$ attains $\delta(s_d | s_{I(d)}) = 1$ and all other $s'_d \in S_d \setminus \{s_d\}$ attain $\delta(s'_d | s_{I(d)}) = 0$. States $s_v \in S_v$ of a value node $v \in N^V$ represent different outcomes that have a utility value $u(s_v)$ associated with them. The total utility is calculated as a sum over the different value nodes $\sum_{v \in N^V} u(s_v)$.

The influence diagram of the pig farm problem is presented in Figure 1. In the diagram, nodes H_i are chance nodes representing the health status of the pig; chance nodes T_i represent the test result, which is conditional on the health status of the pig; decision nodes D_i represent treatment decisions; finally, value nodes V_i , for $i \leq 3$, represent treatment costs and the value node V_4 represents the pig’s market price.

The solution of an influence diagram is a decision strategy that optimizes the desired metric, typically expected utility, at the value nodes. A common additional assumption is perfect recall, meaning that previous decisions can be recalled in later stages. Under this assumption, the optimal decision strategy may be obtained by arc reversals and node removals [23] or dynamic programming [25], for example.

Perfect recall is a rather strict assumption and in many applications, it does not hold. This challenge is circumvented with limited memory influence diagrams [16]. Many algorithms for finding the decision strategy that maximizes the expected utility have been developed, such as the single policy update [16], multiple policy updating [17], branch and bound search [12] and the aforementioned methods converting the influence diagram to a MI(L)P [20, 22].

2.3. Rooted Junction Trees

To achieve a MIP formulation for the decision problem, its influence diagram $G = (N, A)$ must first be transformed into a directed tree called a *gradual rooted junction tree* (RJT) $\mathcal{G} = (\mathcal{V}, \mathcal{A})$ composed of *clusters* $C \in \mathcal{V}$, which are subsets of the nodes of the ID (i.e., $C \subseteq N$) and directed arcs \mathcal{A} connecting the clusters so that each cluster only has one parent. In an influence diagram, the set of nodes N consists of individual chance events, decisions and consequences, while the clusters in \mathcal{V} comprise multiple nodes, hence the notational distinction between N and \mathcal{V} . Starting from an influence diagram, we create an RJT guided by Definition 2.1, which states its necessary properties.

Definition 2.1. A directed rooted tree $\mathcal{G} = (\mathcal{V}, \mathcal{A})$ consisting of clusters $C \in \mathcal{V}$ of nodes $j \in N$ is a gradual rooted junction tree corresponding to the influence diagram G if

- (a) given two clusters C_1 and C_2 in the junction tree, any cluster C on the unique undirected path between C_1 and C_2 satisfies $C_1 \cap C_2 \subseteq C$;
- (b) each cluster $C \in \mathcal{V}$ is the root cluster of exactly one node $j \in N$ (that is, the root of the subgraph induced by the clusters with node j) and all nodes $j \in N$ appear in at least one of the clusters;
- (c) and, for each cluster, $I(j) \in C_j$, where C_j is the root cluster of $j \in N$.

A rooted tree satisfying part (a) in Definition 2.1 is said to satisfy the *running intersection property*. In addition, as a consequence of part (b), we see that an RJT has as many clusters as the original influence diagram has nodes, and each node $j \in N$ can be thought as corresponding to one of the clusters $C \in \mathcal{V}$. As such, we refer to clusters using the corresponding nodes $j \in N$ in the influence diagram as the *root cluster* of node $j \in N$, which is denoted as $C_j \in \mathcal{V}$. Property (c) ensures that the conditional probability of a chance node and the decision strategy of a decision node can be evaluated from its root cluster.

The RJT is created by an algorithm $f : (N, A) \rightarrow (\mathcal{V}, \mathcal{A})$. Any algorithm that creates an RJT satisfying the properties in Definition 2.1 can be used to derive the MIP formulation. In [20], the authors present two alternatives for f . The first algorithm uses a given topological ordering of the nodes and builds the RJT starting from the last cluster and proceeding in the reverse direction of this topological ordering. This algorithm returns an RJT with minimal clusters given the ordering of nodes. The second algorithm has an additional step of finding a “good” topological ordering that results in an RJT with minimal treewidth. For simplicity, we chose to use the algorithm requiring a topological ordering. Using $H_1, T_1, D_1, V_1, H_2, \dots, H_4, V_4$ as a topological ordering, the pig farm influence diagram in Figure 1 is transformed to the gradual RJT in Figure 2.

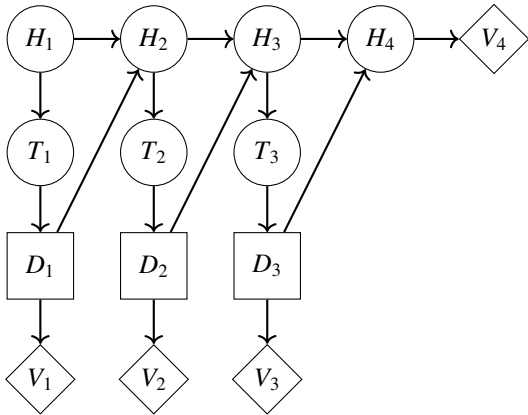


Figure 1: The pig farm problem [16].

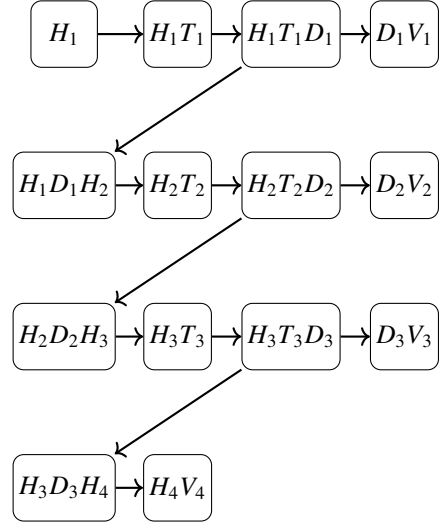


Figure 2: Gradual RJT of the pig farm problem.

Formulating an optimization model based on the RJT representation starts by introducing a vector of moments μ_{C_j} for each cluster C_j , $j \in N$. Parmentier et al. [20] show that for RJTs, we can impose constraints so that these become moments of a distribution μ_N that factorizes according to $G(N, A)$. The joint distribution \mathbb{P} is said to factorize [14] according to G if

$$\mathbb{P}(s_N) = \prod_{j \in N} \mathbb{P}(s_j | s_{I(j)}). \quad (1)$$

In the formulation, $\mu_{C_j}(s_{C_j})$ represents the probability of the nodes within the cluster C_j being in states s_{C_j} and part (c) of Definition 2.1 ensures that $\mathbb{P}(s_j | s_{I(j)})$ can thus be obtained from $\mu_{C_j}(s_{C_j})$ for each $j \in N$. The resulting MIP model is

$$\max \sum_{j \in N^V} \sum_{s_{C_j} \in S_{C_j}} \mu_{C_j}(s_{C_j}) u_{C_j}(s_{C_j}) \quad (2)$$

$$\text{s.t.} \sum_{s_{C_j} \in S_{C_j}} \mu_{C_j}(s_{C_j}) = 1, \forall j \in N \quad (3)$$

$$\sum_{\substack{s_{C_i} \in S_{C_i}, \\ s_{C_i \cap C_j} = s'_{C_i \cap C_j}}} \mu_{C_i}(s_{C_i}) = \sum_{\substack{s_{C_j} \in S_{C_j}, \\ s_{C_i \cap C_j} = s'_{C_i \cap C_j}}} \mu_{C_j}(s_{C_j}), \quad \forall (C_i, C_j) \in \mathcal{A}, s'_{C_i \cap C_j} \in S_{C_i \cap C_j} \quad (4)$$

$$\mu_{C_j}(s_{C_j}) = \mu_{\bar{C}_j}(s_{\bar{C}_j}) p(s_j | s_{I(j)}), \forall j \in N^C \cup N^V, s_{C_j} \in S_{C_j} \quad (5)$$

$$\mu_{C_j}(s_{C_j}) = \mu_{\bar{C}_j}(s_{\bar{C}_j}) \delta(s_j | s_{I(j)}), \forall j \in N^D, s_{C_j} \in S_{C_j} \quad (6)$$

$$\mu_{C_j}(s_{C_j}) \geq 0, \forall j \in N, s_{C_j} \in S_{C_j} \quad (7)$$

$$\delta(s_j | s_{I(j)}) \in \{0, 1\}, \forall j \in N^D, s_j \in S_j, s_{I(j)} \in S_{I(j)}. \quad (8)$$

The formulation (2)-(8) is an expected utility maximization problem where u_{C_j} in the objective function (2) represents the utility values associated with different realizations of the nodes

within the cluster C_j , and $\bar{C}_j = C_j \setminus \{j\}$ is used in constraints (5) and (6) for notational brevity. The decision variables in the model are δ and μ , whereas u and p are parameters that can be pre-calculated. Constraints (3) and (7) state that the variables μ_{C_j} must represent valid probability distributions, with nonnegative probabilities summing to one.

Constraint (4) enforces local consistency between adjacent clusters, meaning that for a pair C_i, C_j of adjacent clusters, the marginal distribution for the nodes in both C_i and C_j (that is, $C_i \cap C_j$) must be the same when obtained from either C_i or C_j .

To ease the notation, moments $\mu_{\bar{C}_j}(s_{\bar{C}_j}) = \sum_{s_j \in S_j} \mu_{C_j}(s_{C_j})$ are used in constraints (5) and (6). The expression $\mu_{\bar{C}_j}$ represents the marginal distribution for cluster C_j with the node j marginalized out. The value $p(s_j | s_{I(j)})$ is the conditional probability of a state s_j given the information state $s_{I(j)}$ and $\delta(s_j | s_{I(j)})$ the decision strategy in node $j \in N^D$. In [20], the authors note that the feasibility of the decision strategy is implied by constraints (3)-(8). Constraint (6) enforces that $\mu_{C_j}(s_{C_j})$ either take value 0 or $\mu_{\bar{C}_j}(s_{\bar{C}_j})$, depending on the decided strategy. It should be noted that constraint (6) involves a product of two variables, and is thus not linear. Since we are limiting ourselves to settings with deterministic strategies (i.e., $\delta(s_d | s_{I(d)}) : S_{I(d)} \times S_d \rightarrow \{0, 1\}$), these constraints become indicator constraints and can be efficiently handled by solvers such as Gurobi [9]. We remark that this would not be the case for more general strategies of the form $\delta(s_d | s_{I(d)}) : S_{I(d)} \times S_d \rightarrow [0, 1]$.

The number of constraints (4)-(6) grows exponentially with respect to the number of nodes within a single cluster. This highlights the need to find a gradual RJT representation where the clusters are as small as possible.

3. Our contributions

3.1. Extracting the utility distribution

For problems with multiple value nodes, e.g., multi-stage decision problems, the expected utility has the property that the total expected utility is the sum of expected utilities in each value node. This property can be exploited in the solution process, and for this reason, many solution methods for influence diagrams, including the RJT approach in [20], only tackle maximum expected utility (MEU) problems.

In contrast, risk measures (such as CVaR) require that the full probability distribution of the consequences is explicitly represented in the model. However, such representations are lost when the value nodes are placed in separate clusters, as in Figure 2, since probability distributions are only defined for each cluster separately. For example, in the pig farm problem described in Section 2.1, the joint distribution of V_1 and V_2 cannot be inferred from the probability distributions of clusters C_{V_1} and C_{V_2} , as we cannot assume the probabilities of consequences in V_1 and V_2 to be independent.

The issue can be circumvented by generating the RJT based on an alternative equivalent influence diagram $\bar{G} = (\bar{N}, \bar{A})$ that collects all consequences under a single value node. We present Algorithm 1, which transforms an influence diagram

into a single-value-node diagram that is equivalent to the original influence diagram in terms of how joint probabilities and utilities are calculated. First, we formalize the notion of equivalence between influence diagrams in Definition 3.1.

Definition 3.1. We say that two influence diagrams $G_1 = (N_1, A_1)$ and $G_2 = (N_2, A_2)$ are equivalent if

- (a) G_1 and G_2 share the same chance and decision nodes, and arcs to these nodes.
- (b) There exists a bijection $g : S_{N_1} \rightarrow S_{N_2}$ such that for any $\delta(s_d | s_{I(d)})$, $\forall d \in N^D$, the following holds: $\prod_{n \in N_1} \mathbb{P}(s_n | s_{I(n)}) = \prod_{n \in N_2} \mathbb{P}(\bar{s}_n | \bar{s}_{I(n)})$ and $\sum_{v \in N_1^V} u(s_v) = \sum_{v \in N_2^V} u(\bar{s}_v)$, where $\bar{s} = g(s)$ for each $s \in S_{N_1}$.

Part (b) in Definition 3.1 implies that for each possible state combination of value nodes from one diagram (say, G_1), an equivalent combination in the other diagram (G_2) that evaluates to the same probability and utility must exist. For instance, if a diagram G_1 has two value nodes with two states each, an equivalent influence diagram G_2 could have one value node with four states that correspond to all possible combinations of the two value nodes in G_1 .

Algorithm 1 Single-value-node conversion

- 1: **Require** $G = (N, A)$
 - 2: **Initialize** $\bar{G} = (\bar{N} = \emptyset, \bar{A} = \emptyset)$
 - 3: Add $N^C \cup N^D$ to \bar{N}
 - 4: Set $\mathbb{P}_{\bar{G}}(s_j | s_{I(j)}) = \mathbb{P}_G(s_j | s_{I(j)})$, $\forall j \in N^C$
 - 5: Add $\{(a, b) \in A \mid b \in N^C \cup N^D\}$ to \bar{A}
 - 6: Create node \bar{v} such that $S_{\bar{v}} = \times_{v \in N^V} S_v$, add $\bar{v} \in \bar{N}$
 - 7: Add (a, \bar{v}) to A for each $a \in I(v)$ such that $v \in N^V$
 - 8: Set $u(s_{\bar{v}}) = \sum_{v \in N^V} u(s_v)$
 - 9: Set $\mathbb{P}(s_{\bar{v}} | s_{I(\bar{v})}) = \prod_{v \in N^V} \mathbb{P}(s_v | s_{I(v)})$
 - 10: **Return** \bar{G}
-

Proposition 3.2. Let $G = (N, A)$ be an influence diagram with $|N^V| > 1$. An influence diagram $\bar{G} = (\bar{N}, \bar{A})$ constructed using Algorithm 1 is equivalent (cf. Definition 3.1).

Proof. See Appendix A. □

When applying Algorithm 1 and transforming the influence diagram into an RJT, according to Definition 2.1, part (c), we have that $\bigcup_{v \in V} I(v) \subset C_{\bar{v}}$, where \bar{v} represents the unique value node in the new diagram. Consequently, the marginal probability distribution $\mu_{C_{\bar{v}}}$ contains information on the joint probability distribution of the consequences $\mathbb{P}(s_{\bar{v}} | s_{I(\bar{v})})$ and this can be used to expose the probability distribution of the utility values. Following this approach, the modified influence diagram of the pig farm problem is presented in Figure 3 and the corresponding gradual RJT in Figure 4.

However, this incurs in computationally more demanding versions of model (2)-(8). In the single-value-node version of the pig farm problem, all decision nodes D_k , $k = 1, 2, 3$, are in the information set of \bar{V} . It follows from the running intersection property that D_k must be contained in every cluster that is

in the undirected path between C_{D_k} and $C_{\bar{V}}$. Therefore, the clusters become larger as the parents of value nodes are “carried over”, instead of evaluating separable components of the utility function at different value nodes. As discussed in [20], this increases the computational complexity of the resulting model.

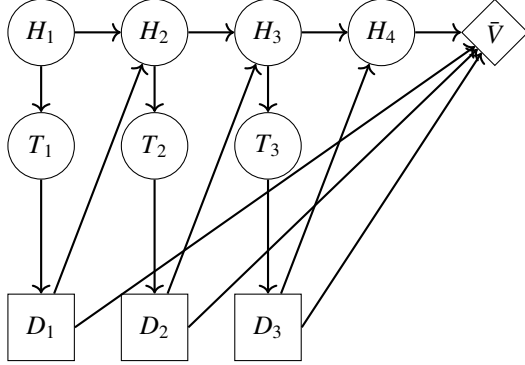


Figure 3: The pig farm problem reformulated ID.

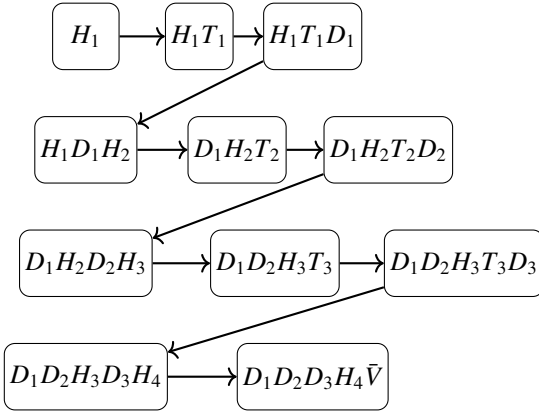


Figure 4: Gradual RJT of the reformulated pig farm problem.

3.2. Modifying the RJT

A single-value-node influence diagram guarantees that the full probability distribution of the consequences can be exposed in the MIP model to optimize or constrain different risk metrics. However, decision-makers may not only be interested in imposing risk constraints on consequences. For instance, in the pig farm problem, the farmer may want to impose chance constraints to ensure that pigs stay healthy throughout the breeding period with a certain likelihood. This requires that the joint probability distribution of the health states of a pig in all periods is available. That is, one needs an RJT that has a cluster containing all health status nodes H_1, \dots, H_4 , which is not found in the RJTs created with algorithms in [20] or with Algorithm 1 (Figures 2 and 4, respectively).

A way to generate a cluster that exposes the desired probability distribution is to directly modify an RJT obtained following [20] while ensuring that the modified RJT fulfills Definition 2.1. Assume that there exists a topological ordering among the nodes of the RJT $\mathcal{G} = (\mathcal{V}, \mathcal{A})$. Suppose one wants to create

a cluster that exposes the joint probability distribution of nodes $M \subseteq N$. Then, one needs to generate an RJT $\bar{\mathcal{G}} = (\bar{\mathcal{V}}, \bar{\mathcal{A}})$ such that $\exists C'_v \in \bar{\mathcal{V}}$ such that $M \subseteq C'_v$. Let \preceq represent a topological order of the nodes N and $\max_{\preceq} M$ return the node with the highest topological order in set M . Let

$$P(C_1, C_k) := \{C_j \in \mathcal{V} \mid \exists (C_1, \dots, C_j, \dots, C_k) \\ \text{with } (C_l, C_{l+1}) \in \mathcal{A}, \forall l \in \{1, \dots, k\}\}$$

be the set of clusters that are contained on any directed path between clusters C_1 and C_k (including themselves). Let $F(j) := \{k \in N \mid P(C_j, C_k) \neq \emptyset\}$ be the set of nodes, whose root cluster can be reached via a directed path starting from cluster C_j . Then, Algorithm 2 leads to an RJT with the desired structure.

Algorithm 2 RJT modification

- 1: **Require** $M \subseteq N$
- 2: **Initialize** $\bar{\mathcal{G}} = (\bar{\mathcal{V}}, \bar{\mathcal{A}})$ equal to \mathcal{G} and denote C'_n as the root cluster of $n \in N$ in $\bar{\mathcal{G}}$
- 3: Find $m = \max_{\preceq} M$
- 4: **For** $n \in M \setminus \{m\}$ such that $n \notin C_m$ **do**:
- 5: **If** $m \notin F(n)$
- 6: Find $e = \max_{\preceq} \{j \in N \mid n, m \in F(j)\}$
- 7: Find $g \in N$ such that $(C_e, C_g) \in \mathcal{A}, m \in F(g), n \notin F(g)$
- 8: Add $C'_e \cap C'_g \in C'_e, \forall C'_e \in P(C_e, C_n)$
- 9: Set $(C'_e, C'_g) \notin \bar{\mathcal{A}}, (C'_n, C'_g) \in \bar{\mathcal{A}}$
- 10: Set $n \in C'_a, \forall C'_a \in P(C'_n, C'_m)$
- 11: **Return** $\bar{\mathcal{G}}$

Proposition 3.3. Assume that an RJT $\mathcal{G} = (\mathcal{V}, \mathcal{A})$ satisfies Definition 2.1. The RJT $\bar{\mathcal{G}} = (\bar{\mathcal{V}}, \bar{\mathcal{A}})$ generated from \mathcal{G} using Algorithm 2 satisfies Definition 2.1.

Proof. See Appendix A □

As an example, we can apply Algorithm 2 to the RJT in Figure 2, which is created by an algorithm given in [20], to include a cluster that contains nodes H_1, \dots, H_4 . The output of Algorithm 2 is the diagram presented in Figure 5. The cluster that exposes the desired joint probability distribution for nodes H_1, \dots, H_4 is the root cluster of H_4 . A more detailed example of applying Algorithm 2 can be found in Appendix A.

3.3. Imposing chance, logical, and budget constraints

Our proposed developments allow one to expose the joint probability distribution of any combination of nodes in the influence diagram, which in turn, enables the formulation of a broad range of risk-aversion-related constraints.

Chance constraints for the joint probability of nodes $M \subseteq N$ can be imposed on the marginal probability distribution of a cluster C_n such that $M \subseteq C_n$. If no such cluster exists in the generated RJT, a suitable cluster can be created with Algorithm 2, or regenerating the RJT based on an influence diagram created with Algorithm 1 if M only contains value nodes and their

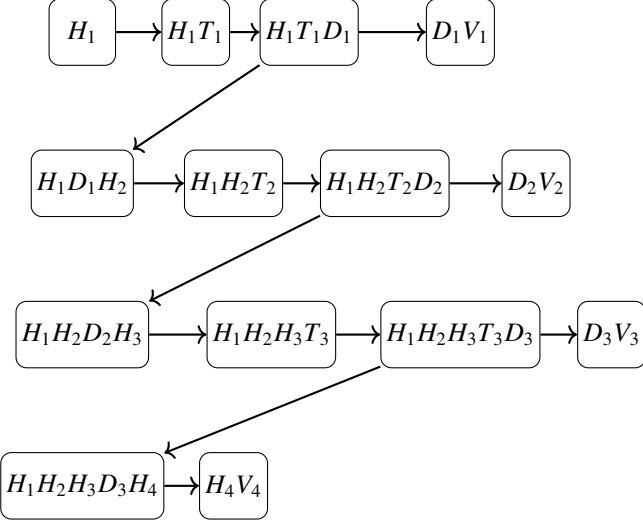


Figure 5: Gradual rooted junction tree for pig farm problem with a cluster that contains nodes H_1, \dots, H_4

parents. Then, chance constraints can be imposed as follows:

$$\sum_{s_{C_n} \in \{S_{C_n} | s_{C_n} \in S_n^o\}} \mu(s_{C_n}) \leq p, \quad (9)$$

where S_n^o is the set of outcomes that the decision maker wishes to constrain and $p \in [0, 1]$ represents a threshold. For instance, assume that a decision-maker wishes to enforce that the probability of the payout of the process being less than some fixed limit b is at most p . Then, a suitable RJT can be generated based on an influence diagram created with Algorithm 1. Constraints can then be enforced for the root cluster of the single value node $C_{\bar{v}}$ and $S_{\bar{v}}^o$ would contain all states $s_{\bar{v}}$ such that $U(s_{\bar{v}}) < b$.

Note that this formulation can be enforced for any cluster C_k such that $M \subseteq C_k$. In addition, to keep the number of variables in the constraint to a minimum, one should choose the smallest of such clusters, i.e., cluster $k' = \arg \min_{k \in N} \{|C_k|, M \subseteq C_k\}$.

Logical constraints can be seen as a special case of chance constraints. For example, in the pig farm problem (in Section 2), the farmer may wish to attain an optimal decision strategy while ensuring that the number of injections is at most two per pig due to, e.g., potential side effects. Then, $S_{\bar{v}}^o$ would contain all realizations of the nodes in $C_{\bar{v}}$ that would lead to a violation of the constraint, i.e., the state combinations in which three injections would be given to a pig. In that case, constraint (10) that makes these scenarios infeasible could be imposed.

$$\sum_{s_{C_{\bar{v}}} \in \{S_{C_{\bar{v}}} | s_{\bar{v}} \in S_{\bar{v}}^o\}} \mu(s_{C_{\bar{v}}}) \leq 0. \quad (10)$$

Budget constraints are analogous to logical constraints, as the farmer could instead have an injection budget, say 200 DKK per pig. Then, $S_{\bar{v}}^o$ should contain all states $s_{\bar{v}}$, where more than 200 DKK is used for treating a pig, with the constraint enforced similarly as in (10).

3.4. Conditional Value-at-Risk

In addition to a number of risk constraints, the proposed reformulations also enable the consideration of alternative risk measures. Next, we focus our presentation on how to maximize conditional value-at-risk. However, we highlight that other risk metrics such as absolute or lower semi-absolute deviation [22] can, in principle, be used. The entropic risk measure [7] can also be used as a constraint. However, incorporating it in the objective function will introduce nonlinearity in the model due to the logarithmic nature of the measure.

The proposed formulation for conditional value-at-risk maximization is analogous to the method developed for decision programming in [22]. It assumes that the joint probability distribution of utility values is available, and hence an RJT generated based on the single-value-node representation of the influence diagram is sufficient for generating a suitable cluster. Denote the possible utility values with $u \in U$ and suppose we can define the probability $p(u)$ of attaining a given utility value. In the presence of a single value node, we would define $p(u) = \sum_{s_{C_v} \in \{S_{C_v} | U(s_{C_v}) = u\}} \mu(s_{C_v})$ and pose the constraints

$$\eta - u \leq M\lambda(u), \quad \forall u \in U \quad (11)$$

$$\eta - u \geq (M + \epsilon)\lambda(u) - M, \quad \forall u \in U \quad (12)$$

$$\eta - u \leq (M + \epsilon)\bar{\lambda}(u) - \epsilon, \quad \forall u \in U \quad (13)$$

$$\eta - u \geq M(\bar{\lambda}(u) - 1), \quad \forall u \in U \quad (14)$$

$$\bar{\rho}(u) \leq \bar{\lambda}(u), \quad \forall u \in U \quad (15)$$

$$p(u) - (1 - \lambda(u)) \leq \rho(u) \leq \lambda(u), \quad \forall u \in U \quad (16)$$

$$\rho(u) \leq \bar{\rho}(u) \leq p(u), \quad \forall u \in U \quad (17)$$

$$\sum_{u \in U} \bar{\rho}(u) = \alpha \quad (18)$$

$$\lambda(u), \bar{\lambda}(u) \in \{0, 1\}, \quad \forall u \in U \quad (19)$$

$$\rho(u), \bar{\rho}(u) \in [0, 1], \quad \forall u \in U \quad (20)$$

$$\eta \in \mathbb{R}, \quad (21)$$

where α is the probability level in VaR_α . Table 1 describes which values the decision variables take due to the constraints (11)-(21).

Variable	Value
η	VaR_α
$\lambda(u)$	1 if $u < \eta$
$\bar{\lambda}(u)$	0 if $u > \eta$
$\rho(u)$	0 if $\lambda(u) = 0$, $p(u)$ otherwise
$\bar{\rho}(u)$	$\begin{cases} p(u) & \text{if } u < \eta, \\ \alpha - \sum_{u \in U} p(u) & \text{if } u = \eta, \\ 0 & \text{if } u > \eta \ (\bar{\lambda}(u) = 0) \end{cases}$

Table 1: Variables and the corresponding values that satisfy (11)-(20)

In constraints (11)-(20), M is a large positive number and ϵ is a small positive number. The parameter ϵ is used to model strict inequalities, which cannot be directly used in mathematical optimization solvers. For example, $x \geq \epsilon$ is assumed to be equivalent to $x > 0$. In practice, it is enough to set ϵ strictly smaller

than the minimum difference of distinct utility values. In [22], the authors use $\epsilon = \frac{1}{2} \min\{|U(s_{\bar{v}}) - U(s'_{\bar{v}})| \mid |U(s_{\bar{v}}) - U(s'_{\bar{v}})| > 0, s_{\bar{v}}, s'_{\bar{v}} \in S_{\bar{v}}\}$. When $\lambda(u) = 0$, constraints (11) and (12) become $-M \leq \eta - u \leq 0$, or $\eta \leq u$. When $\lambda(u) = 1$, they instead become $\epsilon \leq \eta - u \leq M$, or $\eta > u$. Constraints (13) and (14) can be examined similarly to obtain the results in Table 1.

The correct behavior of variables $\rho(u)$ is enforced by (16) and (17). If $\lambda(u) = 0$, constraint (16) forces $\rho(u)$ to zero. If $\lambda(u) = 1$, then $\rho(u) = p(u)$. Finally, assuming η is equal to VaR_{α} and $\rho(u)$ equal to $p(u)$ for all $u < \eta$, the value of $\bar{\rho}(u)$ must be $\alpha - \sum_{u \in U} \rho(u)$ for $u = \eta$. It is easy to see that η must be equal to VaR_{α} for there to be a feasible solution for the other variables. For an equivalence proof, see Salo et al. [22, Appendix A].

By introducing constraints (11)-(20), the CVaR_{α} can then be obtained as $\frac{1}{\alpha} \sum_{u \in U} \bar{\rho}(u)u$. This can be either used as in the objective function or as a part of the constraints of the problem. We also note that the described approach is very versatile in that u can be selected to be, e.g., a stage-specific utility function, thus allowing us to limit risk in specific stages of a multi-stage problem. Krokmal et al. [15] discusses the implications of stage-wise CVaR-constraints in detail.

4. Computational experiments

To assess the computational performance of the model (2)-(8), we use the pig farm problem described earlier. We compare two different versions of the pig farm problem: one with the RJT formulation and the other with the decision programming formulation from [10]. An additional computational example and an analysis of the resulting model sizes from each formulation can be found in Appendix A. All problems were solved using a single thread on an Intel E5-2680 CPU at 2.5GHz and 16GB of RAM, provided by the Aalto University School of Science "Science-IT" project. The models were implemented using Julia v1.10.3 [1] and JuMP v1.23.0 [5] and solved with the Gurobi solver v11.0.2 [9]. The code and data used in this section are available at www.github.com/gamma-opt/risk-averse-RJT.

4.1. Risk-averse pig farm problem

A risk-averse version of the pig farm problem, which maximizes conditional value-at-risk for a confidence level of $1 - \alpha = 0.85$ is solved for different numbers of breeding periods. We use the RJT based on the single-value-node influence diagram from Figure 4 to create the optimization model and add the constraints described in Section 3.4 to represent CVaR. The solution times using our RJT-based formulation are compared to the solution times derived using the decision programming formulation from [10]. For practical reasons, we solve the same single-value-node version of the pig farm problem to compare the solutions. In practice, decision programming can maximize CVaR in influence diagrams with any number of value nodes. However, decision programming creates the exact same MILP model regardless of the number of value nodes.

The solution times of 50 randomly generated instances of the risk-averse pig farm problem with different sizes are presented

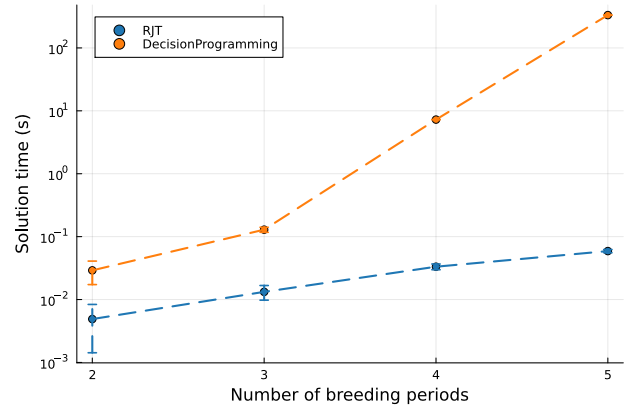


Figure 6: Mean solution times and standard deviations (bars) for 50 random instances in the risk-averse pig farm problem with 2-5 breeding periods on a logarithmic scale.

in Figure 6. The RJT-based formulation consistently offers better computational performance than decision programming for the pig farm problem. In larger pig farm instances, the RJT-based formulation is three orders of magnitude faster than the decision programming formulation. However, the RJT-based formulation still grows exponentially with respect to the number of breeding periods, which could result in computational challenges for larger instances. Still, this exponential growth of the RJT model can be seen as a worst-case scenario, while many problems, including the original pig farm problem (Figure 1), exhibit treewidth independent of the number of stages. For decision programming, as discussed in [10], the number of constraints is exponential in the number of nodes.

4.2. Chance-constrained pig farm problem

In addition, we analyze the computational performance of our formulations on a chance-constrained version of the pig farm problem with different numbers of breeding periods. We use the RJT in Figure 5 and assign chance constraints to the root cluster of H_4 enforcing that the probability of a pig being ill at any time during the breeding period must be less than 40%. Chance constraints are enforced as described in Section 3.3. In Figure 7, we compare the results by solving the same problem with decision programming [10].

The optimization model created based on RJT solves the chance-constrained problem faster than the corresponding decision programming model. In accordance with the results of the risk-averse pig farm problem, RJT is an order of magnitude faster than the corresponding decision programming model.

5. Conclusions

In this paper, we have described a MIP reformulation of decision problems presented as influence diagrams, originally proposed in [20]. Our main contribution is to extend the modelling framework proposed by Parmentier et al. [20] to embed it with more general modelling capabilities. We illustrate how chance constraints and conditional value-at-risk can be incorporated into the formulation. We demonstrate how suitable rooted

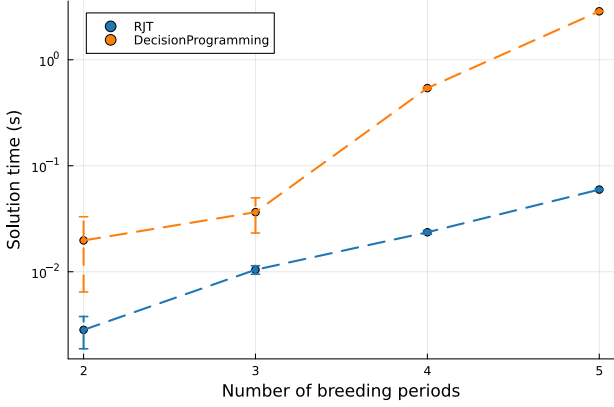


Figure 7: Mean solution times and standard deviations (bars) for 50 random instances in the chance-constrained pig farm problem with 2-5 breeding periods on a logarithmic scale.

junction trees can be generated, either by modifying the underlying influence diagram (Algorithm 1) or directly modifying the rooted junction tree (Algorithm 2).

We show that the model in [20] can be extended beyond expected utility maximization problems to incorporate most of the constraints and objective functions present in decision programming, the alternative MIP reformulation based on LIMIDs described by Salo et al. [22] and Hankimaa et al. [10]. The advantage of using the models described in this paper is that in terms of model size, decision programming models grow exponentially with respect to the number of nodes, whereas the RJT model grows exponentially with respect to treewidth, which is only indirectly influenced by the number of nodes.

We also present computational results, which compare the computational performance of decision programming and our extension of the rooted junction tree model when applied to risk-averse and chance-constrained variants of the pig farm problems. The computational results indicate that risk-averse decision strategies for influence diagrams can be solved considerably faster by using the RJT formulation.

Although this paper furthers the state-of-the-art for MIPs solving risk-averse influence diagrams, typically the resulting MIP is a large-scale model, which in turn limits the size of the problems that can be solved. Hence, future research should concentrate on improving the computational tractability of the MIP model by developing specialized decomposition methods and more efficient formulation.

Appendix A.

This supplementary material contains a more detailed description of Algorithm 2, the proofs for Propositions 3.2 and 3.3 in the manuscript, as well as an additional computational example.

Appendix A.1. Example of applying Algorithm 2

Algorithm 2 is explained using the example RJT presented in Figure A.8. Assume that the topological order of the nodes is

given as follows: $\{A, B, C, D, E, F\}$ and assume that the aim is to modify the RJT by creating a cluster containing nodes A, E and F .

First, Algorithm 2 initializes a new RJT containing the same nodes and arcs. Line 2 of Algorithm 2 finds the last node in M according to the topological order. In the example diagram, it is node F . After running Algorithm 2, cluster C_F , which currently contains nodes B and F , will be the cluster containing nodes A, E and F . Line 3 of the algorithm checks if any of the nodes are already contained in C_F . In the example RJT, only F is contained in C_F . The algorithm will then run the for-loop starting in Line 4 for both A and E . First, consider $n = A$. In Line 5, Algorithm 2 checks if there exists a directed path between C_A and C_F . In the example diagram, such path $p = (C_A, C_B, C_D, C_F)$ exists. Therefore, Algorithm 2 jumps directly to Line 10, in which A is added to all clusters in path p . This results in the RJT in Figure A.9.

Next, the algorithm switches to $n = E$. Now there is no directed path from C_E to C_F in the RJT and therefore Algorithm 2 conducts Lines 6-9. In Line 6, Algorithm 2 searches for a node and its root cluster from which C_F and C_E both can be reached. In the example, there are two potential nodes, A and B . Then, the Algorithm selects the node with maximum topological order, which in this case is B . In Line 7, Algorithm 2 finds a direct predecessor of C_B , which is in a path towards C_F . In the example, the resulting node is D and the corresponding cluster is C_D . This step returns a unique solution because F can only be in one such branch as it has to have a unique root cluster. In Line 8, the algorithm fills clusters on the path between C_B and C_E with nodes contained in both clusters C_B and C_D . This corresponds to nodes A and B . Both are already contained in cluster C_C , whereas A must be added to C_E . This creates an RJT in Figure A.10. In Line 9, Algorithm 2 removes the arc between clusters C_B and C_D and adds an arc between clusters C_E and C_D to create the RJT in Figure A.11. The procedure in Lines 6-9 has now created an RJT with a directed path between clusters C_E and C_F . Finally, Algorithm 2 implements Line 10 and adds E into C_D and C_F to create the RJT in Figure A.12. Then, Algorithm 2 returns an RJT where cluster C_F contains the desired nodes.

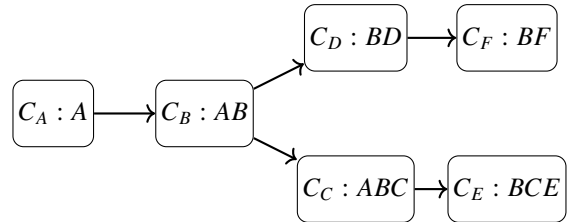


Figure A.8: An example RJT

Appendix A.2. Problem size

From Definition 2.1, we can derive a relationship between the width of the tree and the size of the corresponding model. By definition, a tree with a width k has a maximum cluster C_n containing $k + 1$ nodes. In a gradual RJT, the cluster C_n includes

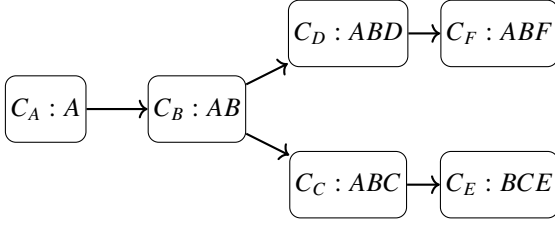


Figure A.9: An RJT after implementing Line 10 for $n = A$

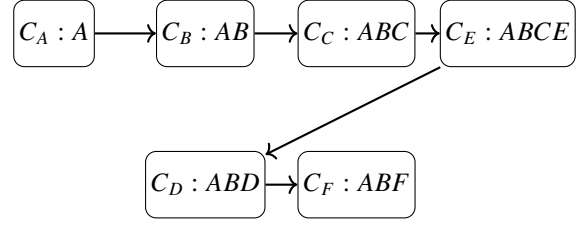


Figure A.11: An RJT after implementing Line 9 for $n = E$

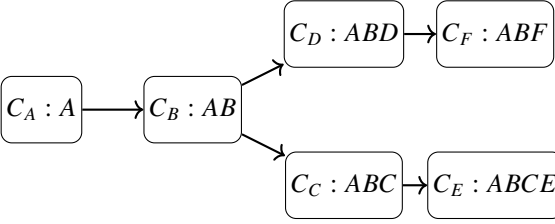


Figure A.10: An RJT after implementing Line 8 for $n = E$

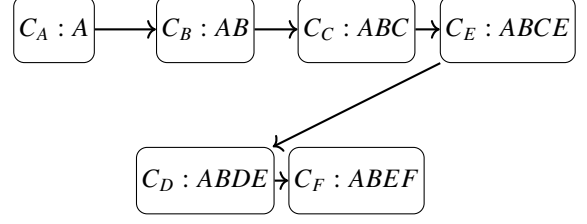


Figure A.12: An RJT after implementing Line 10 for $n = E$

exactly one node $n \in N$ not contained in its parent cluster C_i . Using the running intersection property, the other k nodes in C_n must also be in C_i . Assuming that all nodes $l \in C_i \cup C_n$ have at least two states s_l , this implies that there are $\prod_{l \in C_i \cup C_n} |S_n| \geq 2^k$ local consistency constraints (4) for the pair $(C_i, C_n) \in \mathcal{A}$ and the number of constraints in the model (2)-(8) is thus at least $O(c^k)$, where k is the width of the gradual RJT. This is in line with [20] pointing out that the RJT-based approach is only suited for problems with moderate rooted treewidth.

The width of the tree in Figure 4 (in the manuscript) is $N + 1$, where N is the number of treatment periods in the pig farm problem ($N = 3$ in the example), while the width of the original pig farm RJT in Figure 2 (manuscript) is only 2. Furthermore, we note that the rooted treewidth of a problem is defined as the size of the largest cluster minus one. In an RJT, we have $(I(n) \cup n) \subseteq C_n$ for all $n \in N$ and the treewidth is thus at least $\max_{n \in N} |I(n)|$. For the single-value-node pig farm problem, $|I(\bar{V})| = N + 1$ and for the original pig farm problem, $|I(H_2)| = 2$. Therefore, we conclude that there are no RJT representations for these problems with a smaller width than the ones presented in Figures 2 and 4 (manuscript).

These results imply that the optimization model for the original pig farm problem grows linearly with the number of stages, but the single-value-node pig farm grows exponentially with the number of decisions, suggesting possible computational challenges in larger problems.

Appendix A.3. Proofs

Proof of Proposition 3.2. Consider a state combination $s_N \in S_N$. Let $g(s_N) = s_N$, where $g(s_N)_{\bar{v}} = (s_v)_{v \in N^v}$ and denote $\bar{s}_N = g(s_N)$ for compactness. Notice that the mapping g is a bijection. The utility in graph G is calculated as $\sum_{v \in N^v} u(s_v)$. In graph \bar{G} , the utility is $u(s_{\bar{v}}) = \sum_{v \in N^v} u(s_v)$, which is equivalent to the utility evaluated from graph G . The probabilities are calculated as follows:

$$\begin{aligned}
\mathbb{P}_G(s_N) &= \prod_{c \in N^c, N^v} \mathbb{P}_G(s_c | s_{I(c)}) \prod_{d \in N^d} \delta(s_d | s_{I(d)}) \\
&= \prod_{v \in N^v} \mathbb{P}_G(s_v | s_{I(v)}) \prod_{c \in N^c} \mathbb{P}_G(s_c | s_{I(c)}) \prod_{d \in N^d} \delta(s_d | s_{I(d)}) \\
&= \prod_{v \in N^v} \mathbb{P}_G(s_v | s_{I(v)}) \prod_{c \in \bar{N}^c} \mathbb{P}_{\bar{G}}(\bar{s}_c | \bar{s}_{I(c)}) \prod_{d \in \bar{N}^d} \delta(\bar{s}_d | \bar{s}_{I(d)}) \\
&= \mathbb{P}_{\bar{G}}(\bar{s}_{\bar{v}} | \bar{s}_{I(\bar{v})}) \prod_{c \in \bar{N}^c} \mathbb{P}_{\bar{G}}(\bar{s}_c | \bar{s}_{I(c)}) \prod_{d \in \bar{N}^d} \delta(\bar{s}_d | \bar{s}_{I(d)}) \\
&= \mathbb{P}_{\bar{G}}(\bar{s}_N).
\end{aligned}$$

The second line of the proof follows directly from the first line by separating the chance nodes and value nodes in the first product. The third line of the proof follows directly from Lines 3-5 of Algorithm 1 and the definition of $g(s_N)$. Essentially, chance nodes and decision nodes (as well as their parents) remain the same in both diagrams and therefore, evaluating the product of decision strategy variables and conditional probabilities in chance nodes using the same states must be equivalent. To understand the fourth line of the proof, notice that $\bar{s}_{\bar{v}} = (s_{v_i})_{v_i \in N^v}$, which follows from the definition of $g(s_N)$. In essence, for each possible state combination of value nodes in G , there is a corresponding state for \bar{v} in diagram \bar{G} . The equivalence $\mathbb{P}_{\bar{G}}(\bar{s}_{\bar{v}} | \bar{s}_{I(\bar{v})}) = \prod_{v \in N^v} \mathbb{P}_G(s_v | s_{I(v)})$ follows directly from Line 9 of Algorithm 1. The fifth line is trivial. Hence, the diagrams are equivalent, cf. Definition 3.1.

Proof of Proposition 3.3. Assume that $M \subset N$. Algorithm 2 does not remove any clusters nor remove nodes from any cluster. In addition, if for any $a \in N$, $C_a \subsetneq C'_a$, then it must be that $n \leq a, \forall n \in C'_a \setminus C_a$. Hence, Definition 2.1 (b) and (c) follow directly from the assumption.

Next, property (a) in Definition 2.1 (the running intersection property) is shown to hold for each line of the algorithm separately. Assume that for each line of the algorithm, an RJT

that fulfils the running intersection property is given. In what follows, we will denote C'_c as the root cluster of c before implementing the line defined in Algorithm 2, and C_c^* the cluster after implementing the line defined in Algorithm 2.

Lines 2, 3, 6 and 7 do not modify the RJT at all. For Line 1, Definition 2.1 (a) holds trivially. Also for Line 10, the running intersection property follows directly from the assumption that the junction tree before Line 10 fulfils the running intersection property, since $C'_a \cap C'_b \subset C_a^* \cap C_b^* \subset C_c^* = C'_c \cup \{n\}, \forall C'_c \in P(C'_a, C'_b), C'_a, C'_b \in P(C'_n, C'_m)$.

Line 8 adds $C'_e \cap C'_g$ to every cluster on path $P(C'_e, C'_n)$. Naturally, then for any two clusters of that path $C'_a, C'_b \in P(C'_e, C'_n)$, $C_a^* \cap C_b^* \subseteq \{C'_a \cap C'_b\} \cup \{C'_e \cap C'_g\} \subseteq C_c^*, \forall C_c^* \in P(C_a^*, C_b^*)$. The first subset sign follows from the assumption and definition of Line 8. The second subset sign follows from the fact, that $C'_a \cap C'_b \subset C_c^*$ by assumption and $C'_e \cap C'_g$ is added to C_c^* in Line 8. Therefore, running intersection property holds after implementing Line 8.

For Line 9, consider $C'_a, C'_b \in P(C'_n, C'_m)$ such that $C'_e, C'_g \in P(C'_a, C'_b)$ for e and g as defined in Lines 6 and 7. By assumption, $C'_a \cap C'_b \in C'_c, \forall C'_c \in P(C'_a, C'_b)$, which includes clusters C'_e and C'_g . Therefore, $C'_a \cap C'_b \in C'_e$ and $C'_a \cap C'_b \in C'_g \Rightarrow C'_a \cap C'_b \in C_c^*, \forall C_c^* \in P(C'_e, C'_g)$.

Appendix A.4. Computational examples

Appendix A.4.1. N-monitoring

The N-monitoring problem from [22] represents a problem of distributed decision-making where N decisions are made in parallel with no communication between the decision-makers. The node L in Figure A.13 represents a load on a structure, and nodes R_i are reports of the load, based on which the corresponding fortification decisions A_i are made. The probability of failure in node F depends on the load and the fortification decisions, and the utility in T comprises fortification costs and a reward if the structure does not fail.

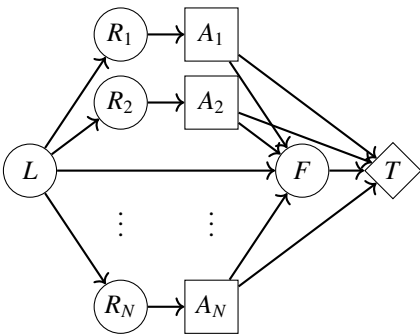


Figure A.13: An influence diagram representing the N-monitoring problem.

With topological order $L, R_1, A_1, \dots, R_N, A_N, F, T$, the rooted junction tree corresponding to the diagram in Figure A.13 is presented in Figure A.14. The structure of parallel observations and decisions in the N-monitoring problem is very different compared to the partially observed Markov decision process (POMDP) structure of the pig farm problem.

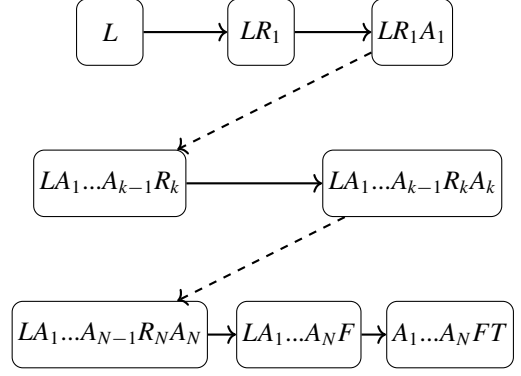


Figure A.14: A rooted junction tree representing the N-monitoring problem.

Any RJT model based on the tree in Figure A.14 has a treewidth of $N + 2$. Decision programming formulations on the other hand scale much better with respect to N compared to the pig farm problem, since only 2 nodes are added to the problem when N is increased by 1, whereas in the pig farm problem, 3 nodes are added.

Fifty randomly generated N-monitoring problem instances maximizing CVaR with probability level $1 - \alpha = 0.85$ are solved with decision programming and the RJT model. This gives insights into the performance of the RJT model compared to decision programming for a problem that does not scale as well for the RJT model. The results are presented in Figure A.15. The results show that the RJT formulation is more efficient in solving the N-monitoring problem. In larger instances, the difference in solution times is approximately 2 orders of magnitude. These results show that even though the structure of the problem would not be optimal for the RJT model, it still outperforms the corresponding decision programming model by a wide margin.

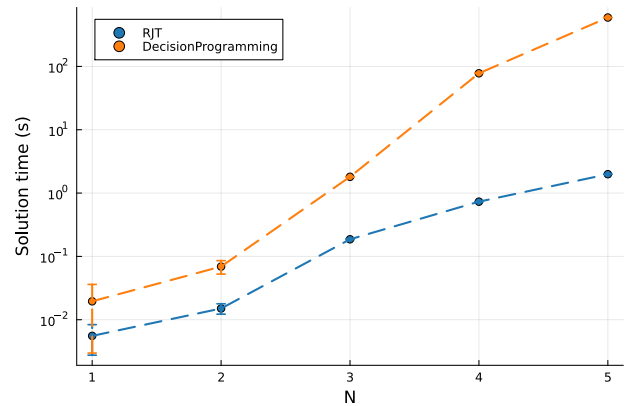


Figure A.15: Mean solution times and standard deviations for 50 random instances of N-monitoring problem

Acknowledgements

This work was supported by the Research Council of Finland (decision 332180). We are also thankful for the contributions from Prof. Ahti Salo and the computer resources from the Aalto University School of Science “Science-IT” project.

References

- [1] Bezanson, J., Edelman, A., Karpinski, S., Shah, V.B., 2017. Julia: A fresh approach to numerical computing. *SIAM Review* 59, 65–98.
- [2] Charnes, A., Cooper, W., 1959. Chance constrained programming. *Management Science* 6, 73–79.
- [3] Cohen, V., Parmentier, A., 2023. Future memories are not needed for large classes of POMDPs. *Operations Research Letters* 51, 270–277.
- [4] Davidson, D., Suppes, P., Siegel, S., 1957. *Decision making; an experimental approach. Decision making; an experimental approach.*, Stanford University Press. Pages: 121.
- [5] Dunning, I., Huchette, J., Lubin, M., 2017. JuMP: A Modeling Language for Mathematical Optimization. *SIAM Review* 59, 295–320.
- [6] Filippi, C., Guastaroba, G., Speranza, M., 2020. Conditional value-at-risk beyond finance: a survey. *International Transactions in Operational Research* 27, 1277–1319.
- [7] Föllmer, H., Knispel, T., 2011. Entropic risk measures: Coherence vs. convexity, model ambiguity and robust large deviations. *Stochastics and Dynamics* 11, 333–351.
- [8] Geissel, S., Sass, J., Seifried, F.T., 2018. Optimal expected utility risk measures. *Statistics & Risk Modeling* 35, 73–87.
- [9] Gurobi Optimization, LLC, 2022. Gurobi Optimizer Reference Manual. URL: <https://www.gurobi.com>.
- [10] Hankimaa, H., Herrala, O., Oliveira, F., Tollander de Balsch, J., 2023. *Decisionprogramming.jl – a framework for modelling decision problems using mathematical programming.* arXiv:2307.13299.
- [11] Howard, R.A., Matheson, J.E., 2005. Influence diagrams. *Decision Analysis* 2, 127–143.
- [12] Khaled, A., Hansen, E.A., Yuan, C., 2013. Solving limited-memory influence diagrams using branch-and-bound search, in: *Uncertainty in Artificial Intelligence (UAI-13)*, AUAI Press, Arlington, Virginia, USA. pp. 331–341.
- [13] Khassiba, A., Bastin, F., Cafieri, S., Gendron, B., Mongeau, M., 2020. Two-stage stochastic mixed-integer programming with chance constraints for extended aircraft arrival management. *Transportation Science* 54, 897–919.
- [14] Koller, D., Friedman, N., 2009. *Probabilistic graphical models: principles and techniques.* MIT press.
- [15] Krokmal, P., Palmquist, J., Uryasev, S., 2002. Portfolio optimization with conditional value-at-risk objective and constraints. *Journal of risk* 4, 43–68.
- [16] Lauritzen, S.L., Nilsson, D., 2001. Representing and solving decision problems with limited information. *Management Science* 47, 1235–1251.
- [17] Mauà, D.D., de Campos, C.P., Zaffalon, M., 2012. Solving limited memory influence diagrams. *Journal of Artificial Intelligence Research* 44, 97–140.
- [18] Homem-de Mello, T., Pagnoncelli, B.K., 2016. Risk aversion in multi-stage stochastic programming: A modeling and algorithmic perspective. *European Journal of Operational Research* 249, 188–199.
- [19] Nielsen, T.D., Jensen, F.V., 2004. Learning a decision maker’s utility function from (possibly) inconsistent behavior. *Artificial Intelligence* 160, 53–78.
- [20] Parmentier, A., Cohen, V., Leclère, V., Obozinski, G., Salmon, J., 2020. Integer programming on the junction tree polytope for influence diagrams. *INFORMS Journal on Optimization* 2, 209–228.
- [21] Rockafellar, R., Uryasev, S., 2000. Optimization of conditional value-at-risk. *Journal of Risk* 2, 21–42.
- [22] Salo, A., Andelmin, J., Oliveira, F., 2022. Decision programming for mixed-integer multi-stage optimization under uncertainty. *European Journal of Operational Research* 299, 550–565.
- [23] Shachter, R.D., 1986. Evaluating influence diagrams. *Operations Research* 34, 871–882.
- [24] Shachter, R.D., Bhattacharjya, D., 2010. Solving influence diagrams: Exact algorithms. *Wiley encyclopedia of operations research and management science*.
- [25] Tatman, J.A., Shachter, R.D., 1990. Dynamic programming and influence diagrams. *IEEE Transactions on Systems, Man, and Cybernetics* 30, 365–379.
- [26] Xu, B., Boyce, S.E., Zhang, Y., Liu, Q., Guo, L., Zhong, P.A., 2017. Stochastic programming with a joint chance constraint model for reservoir refill operation considering flood risk. *Journal of Water Resources Planning and Management* 143.